Clinically Practical Sparse Reconstruction for 4D Prostate DCE-MRI: Algorithm and Initial Experience

Joshua Trzasko[1], Eric Borisch[1], Akira Kawashima[1], Adam Froemming[1], Roger Grimm[1], Armando Manduca[1], Phillip Young[1], and Stephen Riederer[1]
[1]*Mayo Clinic, Rochester, MN, United States*

Target Audience: Scientists and physicians interested in the clinical deployment of sparse reconstruction methods.

Purpose: Prostate cancer is the second-leading cause of cancer death in men in America. Dynamic contrast-enhanced MRI (DCE-MRI) is increasingly used clinically for prostate lesion detection, cancer staging, treatment planning/monitoring, and recurrence detection. However, achieving high spatiotemporal resolution and SNR in 4D (3D+time) prostate DCE-MRI is challenging given the target signal's transiency and gland's medial location. Sparsity-driven image reconstruction [1] is an increasingly popular tool that leverages abstract *a priori* knowledge about the target image(s) to mitigate the tradeoff between resolution and SNR (relative to conventional methods). For prostate, this DCE-MRI may improve precision in cancer characterization and pharmacokinetic modeling. To enable clinically practical sparse reconstruction of 4D DCE-MRI data, we developed an alternating direction method-of-multipliers (ADMM) optimization strategy [2] specifically for our Cartesian acquisition protocol (CAPR [3]) that breaks down this problem in a way that allows many computations to be performed once prior to – rather than repeatedly during – iteration. After overviewing the mechanics of this algorithm, which enables <5 minute 4D DCE-MRI sparse reconstructions, we show that its results were consistently preferred for diagnosis over the clinical standard (SENSE [4]) by radiologists in 19 suspected prostate cancer patient studies.

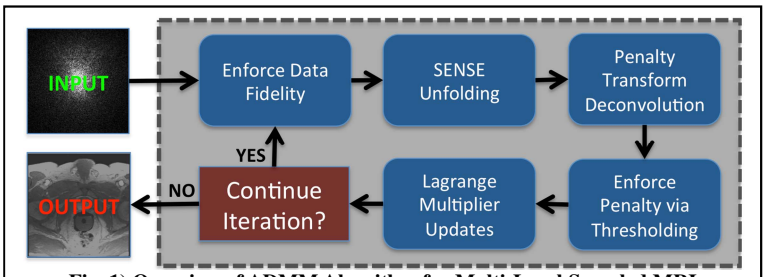

Fig. 1) Overview of ADMM Algorithm for Multi-Level Sampled MRI

Methods: CAPR is a time-resolved ($T \geq 1$), 3D Cartesian acquisition protocol that employs static uniform and dynamic non-uniform undersampling to provide highly accelerated MRI data acquisition. The (pre-whitened) Fourier-domain signal at time index t generated by a CAPR sequence using a C-channel receiver can be modeled as $\mathbf{G}\delta_t = (\mathbf{I}\otimes\mathbf{\Phi_t F})\mathbf{SMX}\delta_t + \mathbf{Z}\delta_t$, where $\mathbf{G}$ is the $KC \times T$ data matrix, $\otimes$ and δ_t are Kronecker's product and delta, $\mathbf{\Phi_t}$ is a $K \times R$ non-uniform binary sampler, $\mathbf{F}$ is an $R \times N$ uniform Fourier sampler, $\mathbf{S}$ is an $NC \times N$ block diagonal coil sensitivity profile matrix, $\mathbf{M}$ is an $N \times M$ binary support matrix, $\mathbf{X}$ is the target $M \times T$ image series, and $\mathbf{Z}$ is proper complex Gaussian noise. Sparse reconstruction of $\mathbf{X}$ from $\mathbf{G}$ can be performed by minimizing the following (multi-penalty) cost functional: $\mathrm{J}(\mathbf{X}) \triangleq \lambda\sum_{b\in\Omega} P(\mathbf{\Gamma_b MX}) + \sum_{t=0}^{T-1}\|(\mathbf{I}\otimes\mathbf{\Phi_t F})\mathbf{SMX}\delta_t - \mathbf{G}\delta_t\|_2^2$, where $\mathbf{\Gamma_b}$ is a linear transform, $P()$ is a sparsity-promoting penalty functional, and $\lambda \geq 0$ is a regularization parameter. ADMM [5] strategies for sparse reconstruction typically decouple the penalty and data fidelity terms in $\mathrm{J}(\mathbf{X})$. We additionally decouple the static ($\mathbf{F}$) and dynamic ($\mathbf{\Phi_t}$) sampling operators [2] by minimizing $\mathrm{J}(\mathbf{W},\mathbf{X},\mathbf{Y},\mathbf{Z}) \triangleq \lambda\sum_{b\in\Omega} P(\mathbf{Z_b}) + \sum_{t=0}^{T-1}\|(\mathbf{I}\otimes\mathbf{\Phi_t})\mathbf{W}\delta_t - \mathbf{G}\delta_t\|_2^2$ jointly over $\mathbf{W},\mathbf{X},\mathbf{Y},\mathbf{Z}$, subject to $\mathbf{W} = (\mathbf{I}\otimes\mathbf{F})\mathbf{SMX}$, $\mathbf{Y} = \mathbf{MX}$, and $(\forall b \in \Omega)\ \mathbf{Z_b} = \mathbf{\Gamma_b Y}$. The ADMM sequence for this problem serially minimizes its (scaled-dual form) augmented Lagrangian with respect to $\{\mathbf{W},\mathbf{X},\mathbf{Y},\mathbf{Z}\}$, and performs three Lagrange multiplier updates every iteration. A high-level overview of this algorithm is presented in Fig. 1. Of note is that $\mathbf{F}$ is time-independent, and SENSE unfolding matrices ($\mathbf{X}$ subproblem) can be precomputed offline (via Cholesky decomposition) [6] prior to iteration for computational economy. Data fidelity and penalty transform inverse operators can also be precomputed. In our current C++ code, raw data is view-shared and Fourier transformed along the frequency-encoding axis before slice-by-slice reconstruction.

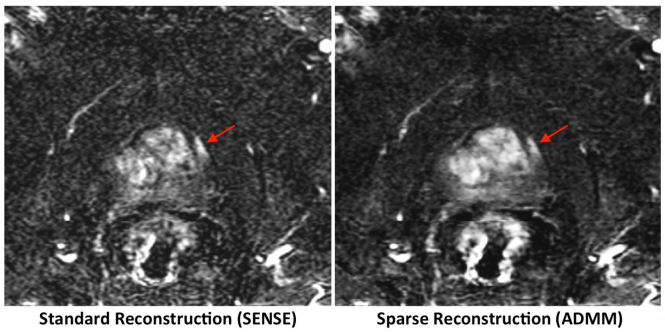

Fig. 2) Example case with suspicious lesion at left anterior horn (arrow)

To assess the performance of the proposed framework, both standard SENSE and ADMM-based sparse reconstruction were run for 19 DCE-MRI studies of consenting suspected prostate cancer patients. Exams were performed at 3T using a 12-channel receiver and CAPR acquisition (TR≈5.7ms; uniform US=2.78x; non-uniform US=4.47x; net US=12.45x; update≈6.6s; frames=55) targeting 256×384×38 volumes with 0.86×0.86×3.0 mm^3 spatial resolution. Post-view-sharing, the temporal footprint of each raw data volume was ≈19.84s and net US=5.52x. Image reconstructions were executed on dual 8-core (Intel Xeon E5-2670, 2.6 GHz) memory workstation with 128 GB. 4D sparse reconstructions (25 iterations) using a 2D total variation penalty were performed in <5 min, with λ set globally based on radiologist preference. Reconstruction results were evaluated by two radiologists in terms of SNR, prostate lesion and prostate/rectal wall delineation, and preferred method for diagnosis. Ordinal scores (>0: sparse reconstruction preferred; =0: no preference; <0: clinical standard preferred) were recorded, and one-sided Wilcoxon sign-rank tests were applied to the radiologists' mean score for each evaluation metric.

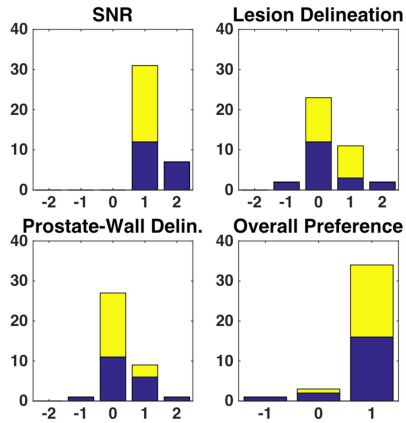

Fig 3. Radiological evaluation results (blue/yellow=reviewer #1/2). Score >0 indicates preference for sparse reconstruction.

Results: Fig. 2 shows representative reconstructions of late-stage axial cross-sections of a 4D DCE-MRI prostate exam. The superior SNR and anatomical delineation offered by ADMM-enabled sparse reconstruction is well-demonstrated near the suspected pathology. Fig. 3 summarizes the radiologists' scores for the exam battery (score vs. count). For each evaluation metric, sparse reconstruction was deemed better than – or preferred over – the standard clinical reconstruction method (p<0.05).

Discussion: We have proposed a novel ADMM algorithm for sparse MRI reconstruction that exploits the specific multi-level sampling structure of our Cartesian acquisition protocol, and demonstrated the performance of – and efficiency enabled by – this strategy for 4D prostate DCE-MRI. Future work will include application of this framework to other DCE-MRI areas (e.g., breast) as well as contrast-enhanced MR angiography (CE-MRA) [7].

Conclusion: ADMM-enabled sparse reconstruction is both practical and preferred for 4D prostate DCE-MRI.

References: [1] Lustig, MRM 2007;58:1182-95 [2] Trzasko, Asilomar SSC 2014;MP8a2-3 [3] Haider, MRM 2008;60:749-60 [4] Pruessmann, MRM 1999;42:942-52 [5] Boyd, FTML 2011;3:1-122, 2011 [6] Borisch, ISMRM 2008:1492 [7] Trzasko, MRM 2011;66:1019-32